



Published in final edited form as:

*J Mech Behav Biomed Mater.* 2019 April ; 92: 90–96. doi:10.1016/j.jmbbm.2019.01.002.

## PVA-Gelatin Hydrogels Formed Using Combined Theta-Gel and Cryo-Gel Fabrication Techniques

Patrick N. Charron<sup>a</sup>, Tess A. Braddish<sup>a</sup>, and Rachael A. Oldinski<sup>a,b,c,d</sup>

<sup>a</sup>Department of Mechanical Engineering, College of Engineering and Mathematical Sciences, University of Vermont, Burlington VT 05405, USA

<sup>b</sup>Bioengineering Program, College of Engineering and Mathematical Sciences, University of Vermont, Burlington VT 05405, USA

<sup>c</sup>Department of Electrical and Biomedical Engineering, College of Engineering and Mathematical Sciences, University of Vermont, Burlington VT 05405, USA

<sup>d</sup>Materials Science Program, Graduate College, University of Vermont, Burlington VT 05405, USA

### Abstract

Poly(vinyl alcohol) (PVA) is a synthetic, biocompatible polymer that has been widely studied for use in bioengineered tissue scaffolds due to its relatively high strength, creep resistance, water retention, and porous structure. However, PVA hydrogels traditionally exhibit low percent elongation and energy dissipation. PVA material and mechanical properties can be fine-tuned by controlling the physical, non-covalent crosslinks during hydrogel formation through various techniques; PVA scaffolds were modified with gelatin, a natural collagen derivative also capable of forming reversible hydrogen bonds. Blending in gelatin and poly(ethylene glycol) (PEG) with PVA prior to solidification formed a highly organized hydrogel with improved toughness and dynamic elasticity. Theta-gels were formed from the solidification of warm solutions and the phase separation of high molecular weight gelatin and PVA from a low molecular PEG porogen upon cooling. While PVA-gelatin hydrogels can be synthesized in this manner, the hydrogels exhibited low toughness with increased elasticity. Thus, theta-gels were additionally processed using cryo-gel fabrication techniques, which involved freezing theta-gels, lyophilizing and rehydrating. The result was a stronger, more resilient material. We hypothesized that the increased formation of physical hydrogen bonds between the PVA and gelatin allowed for the combination of a stiffer material with energy dissipation characteristics. Rheological data suggested significant changes in the storage moduli of the new PVA-gelatin theta-cryo-gels. Elastic modulus, strain to failure, hysteresis and resilience were studied through uniaxial tension and dynamic mechanical analysis in compression.

---

**Publisher's Disclaimer:** This is a PDF file of an unedited manuscript that has been accepted for publication. As a service to our customers we are providing this early version of the manuscript. The manuscript will undergo copyediting, typesetting, and review of the resulting proof before it is published in its final citable form. Please note that during the production process errors may be discovered which could affect the content, and all legal disclaimers that apply to the journal pertain.

Conflicts of interest

There are no conflicts to declare.

## Keywords

material properties; dynamic tests; polyvinyl alcohol; gelatin; mechanical testing; rheology

---

## 1. Introduction

Polymers, more specifically hydrogels, have been studied extensively for biomaterials and tissue engineered scaffolds use due to their wide-ranging physical and mechanical properties, which can be tuned for specific applications via a variety of chemical or material modifications.(1) Polyvinyl alcohol (PVA) is a synthetic polymer often studied for soft tissue replacement and regeneration studies owing to its biocompatibility, high water content, and tunable properties.(1–4) While there are many methods to adjust the mechanical properties of PVA, most of these methods depend on a thermal transition, during which a PVA solution crystallizes through non-covalent intermolecular bonds, resulting in a physically crosslinked polymer network with a microporous structure.(5–9) Theta-gels, PVA hydrogels formed in the presence of a porogen, take on a unique structure, with the lower molecular weight porogen and higher molecular weight PVA separating into two distinct phases during the thermal transition, resulting in enhanced crystallinity in the denser PVA-abundant regions.(10–12) The porogen can later be removed through dialysis, resulting in macro-pores in a rigid PVA network.(11, 12) PVA hydrogels can also be formed through cryo-processing, during which the mechanical properties can be tuned through subsequent freeze-thaw cycles, resulting in cryo-gels.(13–15) During cryo-gel fabrication, the formation and expansion of ice crystals within the PVA solution (or hydrogel for repeated freeze-thaw cycles) results in PVA densification in the material, increasing the overall organization and crystallinity of the material, thus increasing PVA rigidity.

Gelatin, a non-specific derivative of collagen, is a thermoresponsive polymer capable of physical crystallization.(16–18) We hypothesized that an increased formation of hydrogen bonds between PVA and gelatin would allow for increased stiffness while also resulting in a higher toughness and resilience. Here, a PVA-based theta-cryo-gel containing gelatin is presented, utilizing both theta-gel and cryo-gel fabrication techniques, resulting in a tough and resilient supramolecular hydrogel. The addition of low molecular weight polyethylene glycol (PEG) porogen in the PVA and PVA-gelatin solutions provided the phase separation critical to theta-gel formation, while a subsequent freeze-thaw cycle was employed to modify the structure-function material relationship. PVA-gelatin cryo-gels, in the absence of theta-gel processing, were used as experimental controls.

## 2. Materials and methods

### 2.1. PVA-gelatin theta-cryo-gel synthesis

PVA-gelatin theta-cryo-gels (TC-gels) were prepared using a combination of previously reported techniques. Low and high molecular weight PVA [Mw: low = 89–98 kg/mol, high = 145 kg/mol; 99+% hydrolyzed], PEG [Mn = 400 g/mol], and gelatin [bovine derived, type B powder] were purchased from Sigma-Aldrich. PVA (15% w/v), PEG (15% w/v) and/or gelatin (1% w/v) were prepared with DI water and blended together in a round-bottom flask

at 105 °C with the use of a condenser until all of the constituents formed a homogeneous solution. This solution was poured into open-faced 3-mm tall molds and cooled overnight at room temperature, initiating the theta-gel transformation. The molds were then placed in a -20 °C freezer overnight to initiate the cryo-gel transformation. The following day the molds were removed from the freezer and the resulting hydrogels thawed to room temperature. The resulting theta-cryo-gels were purified via dialysis in DI water for 3 days at room temperature. Samples were stored in DI water at 4–8 °C to maintain hydration and prevent gelatin components from breaking down prior to testing.

## 2.2. Hydrogel structure and composition

**2.2.1. Scanning electron microscopy (SEM)**—Prior to imaging, specimens were dried via lyophilization and mounted onto aluminum specimen mounts using conductive carbon tape. Specimens were sputter coated with 3–4 nm gold/palladium. SEM images were obtained using a JEOL JSM 6060 SEM (JEOL Ltd.) operating at an accelerating voltage of 10 keV at varying magnifications.

**2.2.2. Attenuated total reflection Fourier Transform infrared (ATR-FTIR) spectroscopy**—Prior to testing, specimens were dried via lyophilization (FreeZone, Labconco). Spectra were obtained using a FT-IR (IRAffinity-1S, Shimadzu) with an ATR head. Spectra were collected from 800–4000 cm<sup>-1</sup> at a resolution of 8 cm<sup>-1</sup>.

**2.2.3. Swell ratio and water content**—In preparation for equilibrium water content and swell ratio measurements, rectangular hydrogel specimens were lyophilized, following ASTM D2765–11.<sup>(19)</sup> The dehydrated specimens were weighed and a dry weight ( $W_D$ ) was recorded. The specimens were then submerged in DI water at room temperature for 24 hours. The hydrated hydrogels were weighed again and a wet weight ( $W_W$ ) was recorded. Equilibrium water content was calculated as the difference between the wet weight and the initial dry weight, divided by the wet weight. Swell ratio was calculated as the difference between the wet weight and the initial dry weight, divided by the dry weight.

$$\text{Equilibrium Water Content} = \frac{W_W - W_D}{W_W} \times 100\%$$

$$\text{Swelling Ratio} = \frac{W_W - W_D}{W_D} \times 100\%$$

**2.2.4. Van Gieson staining**—To verify the retention of gelatin in the hydrogels after fabrication, TC-gels and control hydrogels (8-mm diameter, 2.97±0.51-mm thick) were placed in Van Gieson solution (Electron Microscopy Sciences) and allowed to equilibrate for 5 minutes. The specimens were removed from the staining solution and rinsed in DI water until no stain leached from scaffolds. The theoretical gelatin content in the hydrogels was either 0 or 1% (w/v) and qualitative verification of these percentages were determined. Color images were captured using a digital camera.

## 2.3. Mechanical testing

**2.3.1. Shear rheometry**—Shear rheology was performed using an AR 2000 rheometer (TA Instruments) at 25 °C, with a Peltier plate and 20-mm diameter stainless steel cone geometry (1°59'06"). Various 20-mm diameter hydrogel samples were prepared and loaded onto the Peltier plate. Oscillatory time sweeps were performed at 1% radial strain and 10 Hz over a period of 3 minutes at 25 °C. (11) Oscillatory temperature sweeps were performed at 1% radial strain and 10 Hz over a temperature range of 25–41 °C (2 °C increments with 1 minute for equilibration). Data were analyzed using analytical software (TA Data Analysis). Shear storage ( $G'$ ) and loss ( $G''$ ) moduli were calculated after 180 seconds.

**2.3.2. Uniaxial tensile test**—Tensile tests were performed on a Discovery hybrid rheometer (TA instrument), using the dynamic mechanical analysis (DMA) machine with a film tension clamp geometry at room temperature. Rectangular films were cut from cast hydrogels to obtain standard samples (15 × 12-mm) with a uniform thickness of 3-mm. Samples were clamped in position and axially strained at a rate of 100  $\mu\text{m/s}$ . Engineering axial stress and strain were calculated from force and displacement data. The tensile elastic modulus (E) was calculated using the linear region (10–60% strain) of the loading curves.

**2.3.3. Uniaxial unconfined compression test**—Uni-axial unconfined compression tests were performed using an AR 2000 rheometer at 25 °C, using a Peltier plate and 8-mm diameter stainless steel plate geometry. TC-gel samples (8-mm diameter,  $2.97 \pm 0.51$ -mm thick) were loaded onto the Peltier plate and a pre-load of 0.01 – 0.03 N was applied. Samples were compressed at 0–20% unconfined axial strain for 1 cycle, and at 5–20% strain for 5 cycles; the axial strain rate was 10  $\mu\text{m/s}$ . Data were analyzed using analytical software (TA Data Analysis). The compressive elastic modulus (E) was calculated using the linear region of the loading curve from the initial cycle of the hysteresis test. The area between the loading and unloading curves from the cyclic hysteresis testing was calculated using a Matlab code and the trapezoidal numerical integration (trapz) function.

## 2.4. Statistics

Swell ratio, equilibrium water content, oscillatory time sweep, compressive moduli, hysteresis area, and elastic moduli are presented as mean  $\pm$  standard deviation (SD). Statistical comparisons were observed between materials within each molecular weight group for the physical characterization. Comparisons were also made between like materials, across molecular weight groups, for the mechanical characterization. Analyses were performed using a t-test with an unpaired one-tailed distribution and two-sample unequal variance (type 2), where  $p < 0.05$  was statistically significant. The goal was to examine the effect of PVA molecular weight and the addition of gelation on the mechanical properties of PVA theta-cryo-gels.

## 3. Results and discussion

### 3.1. TC-gel structure and composition

In this study, we investigated the effect of combined theta- and cryo-gel fabrication processes using varying polymer blend combinations of PVA, PEG, and gelatin to control

hydrogel material and mechanical properties. Hydrogels, comprised of either high or low molecular weight PVA, were fabricated in the presence of PEG (a low molecular weight porogen), gelatin, or a combination of the two. The hydrogels were cooled to complete a theta-gel transition, frozen to complete a cryo-gel transition, and dialyzed to remove the PEG porogen, i.e., the final hydrogels did not contain PEG and the distinction of PEG use in the nomenclature is to signify whether it was used. As reported previously, the use of PEG as a porogen results in macro-porous semi-crystalline PVA networks, as shown in Fig. 1A. (11),(12) ATR-FTIR spectra for the groups containing the high molecular weight PVA are shown in Fig. 1B, along with gelatin and PVA controls. The physical crosslinking of PVA controls and the hydrogels incorporating gelatin occurred due to numerous inter-chain hydrogen bonds between OH groups, formed during crystallization of the polymer and identified as the peak at  $1141\text{ cm}^{-1}$ .(11, 20, 21) The intensity of this peak is related to the C-O stretching vibrations of the intermolecular hydrogen bonds contained within the crystalline regions of PVA. The PVA control shows a large peak at this wavelength compared to the other samples. As expected, there is no peak associated with gelatin at this wavelength. The existence of intermolecular hydrogen bonds was also verified by the appearance of peaks within  $1090 - 1150\text{ cm}^{-1}$ . The PVA and PVA theta-cryo-gel without gelatin display similar curves in this region. Gelatin shows small peaks in this region, representative of the hydrogen bonds in the peptide. However, the PVA theta-gels and PVA cryo-gels which contained gelatin show increased intensity for the C-O peak. The increased peak areas for these samples indicates that hydrogen bonding occurred between PVA and gelatin, which is supported by the increased stiffness of the composite hydrogels (see Fig.2-4). Due to the use of PEG porogens during the solidification process, PVA and gelatin molecules interacted more intensely with each other through the theta-gel and cryo-gel processing, compared to PVA-gelatin cryo-gels, which is supported by the data in Fig. 1B.

The equilibrium water content and swell ratio of PVA, PVA-PEG, and PVA-PEG-gelatin TC-gels are shown in Fig. 1C. The swell ratio decreased with the addition of PEG, and with the combined addition of both PEG and gelatin; the materials with higher amounts of crystalline content resulted in lower swell ratios, as expected. It was previously shown that increasing porogen (i.e., PEG) concentration increased hydrogel pore size and porosity, resulting in higher water contents; however, this trend was only seen with the addition of gelatin in the theta-gels.(10, 22) It has also been shown that the addition of gelatin to PVA theta-gels increased pore size compared to PVA theta-gel controls.(11)

Gelatin retention in the biosynthetic TC-gels was verified using a visual Van Geison assay, as shown in Fig. 1D. Qualitatively, materials with higher molecular weight PVA appear to retain more gelatin, resulting in a darker stain. It was hypothesized that the longer polymer chains of the high molecular weight PVA become more physically entangled with the gelatin polymer chains, resulting in an increased retention of the gelatin component. Similarly, the hydrogel samples fabricated with PEG appear darker after the Van Geison assay. During the theta-transition and pore formation, PVA chains form semi-crystalline regions as the chains are pressed together by forming ice crystals.(7, 13) These regions experience higher degrees of chain entanglement and ionic interactions, resulting in more gelatin being trapped in these systems. Additionally, the helical or coil structure of gelatin may become ensnared between the planar structures of PVA.(23)

## 3.2. Mechanical properties

**3.2.1. Shear rheometry**—Soft tissues can undergo shear loading, thus, shear rheological testing was performed to study the TC-gel response to shear loading events and thermal transitions. Simple oscillatory time sweeps were performed to collect storage and loss moduli at room temperature. As expected, no significant changes in mechanical response as a function of time were observed, indicating a stable hydrogel network was formed (Fig. 2A). The highest shear modulus was obtained by the 15-15-1 groups; the 15-15-1 groups exhibited significantly higher moduli compared to the remaining groups. Varying the PVA molecular weight showed little impact on the final shear mechanical properties, suggesting that the hydrogel fabrication process affected the storage modulus more compared to the PVA chain length. More importantly, the greatest increase in shear stiffness occurred with the TC-gel fabrication process in the presence of gelatin. Without the addition of gelatin, the differences in the cryo-gel and TC-gels was minimal.

Oscillatory temperature sweeps from 25 to 41 °C were used to characterize the hydrogel response to temperatures approaching and exceeding body temperature, as shown in Fig. 2B. Material trends from the oscillatory time sweep were apparent in the temperature sweeps as well. Both 15-15-1 groups were considerably higher than their non-gelatin counterparts, with no significant differences between the remaining groups. As the temperature increased, there was a corresponding drop in shear moduli in the groups containing gelatin, further confirming the presence of the thermo-responsive polymer in the system. This softening is attributed to the conformational change of gelatin from a triple helix structure to a less rigid coil structure.(24, 25) There were no appreciable changes in the moduli for the control groups without gelatin.

**3.2.2. Tensile mechanical properties**—Tensile testing was employed to investigate Young's modulus and percent elongation (i.e., strain to failure) of the hydrogels. Due to testing limitations, the only groups that were able to be successfully loaded for testing were the 15H-15-1 and 15H-15-0 groups. The remaining groups were unable to be clamped into the testing apparatus successfully and failed prior to testing. The group containing gelatin displayed a significantly higher Young's modulus than the group containing just PVA, both fabricated with the PEG porogen ( $279.8 \pm 9.69$  Pa compared to  $179.2 \pm 21.72$  Pa,  $p < 0.01$ ), as shown in Fig. 3A. Further displayed in Fig. 3B, the Young's moduli for both materials were much lower than their corresponding compressive moduli. Interestingly, both materials exhibited percent elongations exceeding 90%; however, there was no significant difference between the groups with or without gelatin ( $112.09 \pm 20.05\%$  compared to  $92.89 \pm 26.56\%$ ,  $p = 0.37$ ), suggesting that the addition of gelatin did not result in further elongation than both the theta- and cryo-processes.

**3.2.3. Compressive mechanical properties**—Hydrogel compressive elastic moduli ranged from  $715.5 \pm 266.5$  Pa for the 15L-0-1 group, up to an impressive  $43092.0 \pm 4705.9$  Pa for the 15H-15-1 group, indicating a high dependence on hydrogel composition and fabrication technique (Fig. 4A). Hydrogels fabricated without PEG exhibited the lowest compressive moduli, while hydrogels fabricated with PEG and containing gelatin demonstrated the highest moduli. Without the PEG porogen, the 15-0-1 groups relied

predominately on chain entanglement and electrostatic forces to form a hydrogel, resulting in a less structured, softer material. Some crystallinity was imbued during the cryo-gel process, wherein the hydrogel was frozen, causing ice crystal formation, forcing polymer chains into more ordered crystals.<sup>(13, 26)</sup> There was a significant increase in stiffness with the use of the PEG porogen, as the porogen induced the PVA polymer chains to form tighter semi-crystalline regions around the water soluble PEG during the cooling process.<sup>(7)</sup> Similar to the previous case, the cryo-gel process reinforced crystallinity through ice formation, further stiffening the 15-15-0 TC-gels. The highest compressive moduli were associated with the 15-15-1 groups, which benefited from both the use of PEG porogens and increased polymer entanglement with the gelatin, thus exhibiting significantly higher moduli than either of the prior groups. The data suggests that increasing the molecular weight of PVA led to increased compressive moduli; however, significant differences between PVA molecular weight groups were only observed in the groups containing gelatin (15-15-1  $p < 0.001$ , 15-15-0  $p = 0.77$ , 15-0-1  $p < 0.05$ ), suggesting that the change in mechanical properties due to the theta-transition, in addition to cryo-processing, was more dominant than altering the molecular weight. The significant differences seen in the groups containing gelatin suggests correlation between increasing chain entanglement<sup>(23)</sup> between PVA and gelatin and increasing PVA molecular weight, resulting in a stiffer network.

Cyclic compressive hysteresis tests were performed in one and 5 cycle iterations to investigate material resilience, and energy dissipation properties, as a result of chain mobility during dynamic loading. Similar to the compression tests results, a wide range of values were obtained depending highly on the hydrogel composition and processing technique, with significant differences seen between groups with similar PVA molecular weights in both 1 cycle and 5 cycle test results (Fig. 4B,C respectively). Groups that did not use PEG were considerably more compliant and weaker due to a lack of theta-transition, with only ice crystal formation of the singular cryo-cycle inducing polymer organization. Groups fabricated with PEG were considerably stiffer, with the groups fabricated with PEG and gelatin exhibiting the highest stresses for similar displacements. These trends were justified, as the materials with higher compressive moduli were able to maintain higher stress values over the same strain values. The area between the loading and unloading curves was calculated to quantify the differences in material groups and to make inferences on energy loss (Fig. 4D). Groups fabricated with the PEG porogen and containing gelatin exhibited the largest area between curves, indicating higher energy dissipation, followed by groups fabricated with PEG, and lastly the groups containing gelatin. The energy loss can be attributed to chain mobility and rearrangement of hydrogen bonds during each cycle.<sup>(27)</sup> Upon the removal of the load, the molecular rearrangement dissipated energy introduced into the material during loading, and the elastic behavior of the polymer chains resulted in excellent dimensional stability upon return, indicated by the absence of plastic deformation and the continued ability to dissipate energy with repetitive loading.<sup>(28)</sup> PVA and gelatin combined in the system increased crystallinity, as shown in Fig. 1B, comprised of physical self-healing hydrogen bonds.<sup>(29)</sup> The supramolecular nature of the composite hydrogel resulted in a material with a high resilience, based on the thermodynamic principles of elastic polymer networks.<sup>(28, 29)</sup> Both constituents affected the overall structure, increasing the resistance of permanent deformation.<sup>(30)</sup> In addition, fluid flow, made easier in the

presence of larger pores, relieved stress by dissipating energy which contributed to the energy dissipation of materials with high swell ratios. These experiments were performed in unconfined compression, allowing unrestricted water flow in and out of the hydrogel network, however, water loss due to evaporation was not prevented.

## Conclusions

The incorporation of gelatin in the fabrication of PVA TC-gels enabled the production of highly resilient, stiff and tough hydrogels. Indeed, the addition of the short chain, thermo-responsive peptide gelatin resulted in an enhanced hydrogel optimal for soft tissue repair, exhibiting statistically significant improvements in mechanical properties compared to PVA alone. The enhanced properties may depend on the incorporation of gelatin into the PVA crystalline structure, increasing the number of physical hydrogen bonds; the reversible bonds combined with elastic, mobile chains enabled tough materials to dissipate energy through molecular motion, however, the materials exhibited high resilience upon unloading as a result of the supramolecular network. As shown in this report, varying the composition and/or fabrication technique of these novel materials allows for the optimization of physical and mechanical properties. Despite being mechanically advantageous for soft tissue replacement, PVA lacks cell adhesion capability. The addition of biomolecules, proteins, or bioactive compounds can be used to impart bio-functionality onto the PVA material.(31–33) It is further hypothesized that the addition of gelatin provides cell adhesion ligands creating a bioactive hydrogel.(11) Future experiments will investigate the efficacy of PVA-gelatin TC-gels for use in biomedical applications via cell adhesion, viability, and migration studies.

## Acknowledgements

This work was funded in part by NIH Grant R01 EB020964–01 (Oldinski) as well as the University of Vermont College of Engineering and Mathematical Sciences.

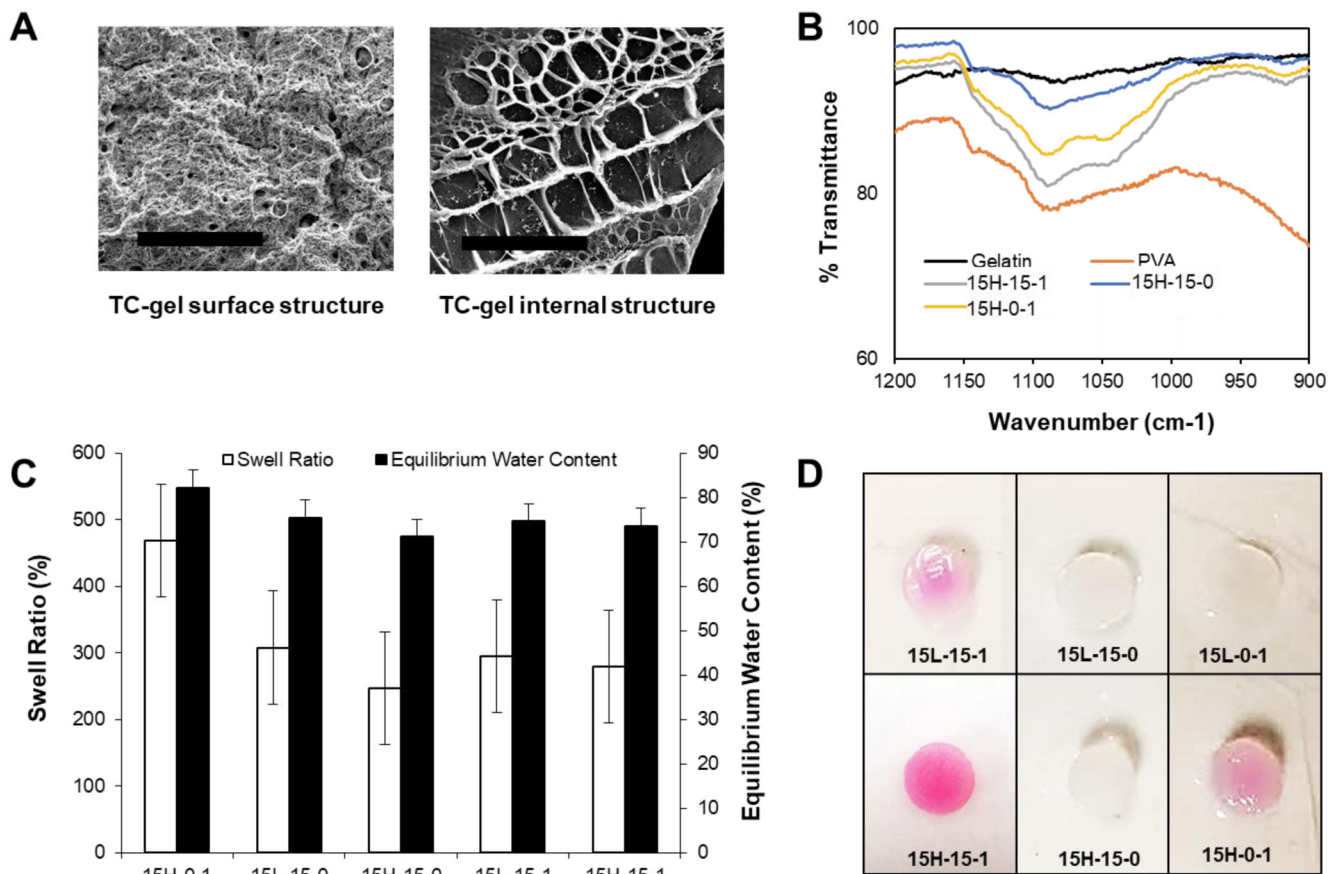
## References

1. Iatridis JC, Nicoll SB, Michalek AJ, Walter BA, Gupta MS. Role of biomechanics in intervertebral disc degeneration and regenerative therapies: what needs repairing in the disc and what are promising biomaterials for its repair? *The Spine Journal*. 2013;13(3):243–62. [PubMed: 23369494]
2. Bryant S, Nuttelman C, Anseth K. The effects of crosslinking density on cartilage formation in photocrosslinkable hydrogels. *Biomedical sciences instrumentation*. 1998;35:309–14.
3. Nuttelman CR, Henry SM, Anseth KS. Synthesis and characterization of photocrosslinkable, degradable poly (vinyl alcohol)-based tissue engineering scaffolds. *Biomaterials*. 2002;23(17):3617–26. [PubMed: 12109687]
4. Martens PJ, Bryant SJ, Anseth KS. Tailoring the degradation of hydrogels formed from multivinyl poly (ethylene glycol) and poly (vinyl alcohol) macromers for cartilage tissue engineering. *Biomacromolecules*. 2003;4(2):283–92. [PubMed: 12625723]
5. Stammen JA, Williams S, Ku DN, Guldborg RE. Mechanical properties of a novel PVA hydrogel in shear and unconfined compression. *Biomaterials*. 2001;22(8):799–806. [PubMed: 11246948]
6. Alves MH, Jensen BE, Smith AA, Zelikin AN. Poly (vinyl alcohol) physical hydrogels: new vista on a long serving biomaterial. *Macromolecular bioscience*. 2011;11(10):1293–313. [PubMed: 21793217]
7. Bodugoz-Senturk H, Choi J, Oral E, Kung JH, Macias CE, Braithwaite G, et al. The effect of polyethylene glycol on the stability of pores in polyvinyl alcohol hydrogels during annealing. *Biomaterials*. 2008;29(2):141–9. [PubMed: 17950839]



8. Bichara DA, Zhao X, Bodugoz-Senturk H, Ballyns FP, Oral E, Randolph MA, et al. Porous poly (vinyl alcohol)-hydrogel matrix-engineered biosynthetic cartilage. *Tissue Engineering Part A*. 2010;17(3-4):301-9. [PubMed: 20799889]
9. Lee S-Y, Wee A-S, Lim C-K, Abbas AA, Selvaratnam L, Merican AM, et al. Supermacroporous poly (vinyl alcohol)-carboxymethyl chitosan-poly (ethylene glycol) scaffold: an in vitro and in vivo pre-assessments for cartilage tissue engineering. *Journal of Materials Science: Materials in Medicine*. 2013;24(6):1561-70. [PubMed: 23512151]
10. Badiger MV, McNeill ME, Graham NB. Porogens in the preparation of microporous hydrogels based on poly (ethylene oxides). *Biomaterials*. 1993;14(14):1059-63. [PubMed: 8312460]
11. Miao T, Miller EJ, McKenzie C, Oldinski RA. Physically crosslinked polyvinyl alcohol and gelatin interpenetrating polymer network theta-gels for cartilage regeneration. *J Mater Chem B*. 2015;3(48):9242-9.
12. Charron PN, Blatt SE, McKenzie C, Oldinski RA. Dynamic mechanical response of polyvinyl alcohol-gelatin theta-gels for nucleus pulposus tissue replacement. *Biointerphases*. 2017;12(2):
13. Peppas NA, Stauffer SR. Reinforced uncrosslinked poly (vinyl alcohol) gels produced by cyclic freezing-thawing processes: a short review. *Journal of Controlled Release*. 1991;16(3):305-10.
14. Lozinsky V, Damshkaln L, Kurochkin I, Kurochkin I. Study of cryostructuring of polymer systems: 28. Physicochemical properties and morphology of poly (vinyl alcohol) cryogels formed by multiple freezing-thawing. *Colloid journal*. 2008;70(2):189-98.
15. Koch ME. Mechanical Optimization Of Poly (vinyl Alcohol) Cryogels To Activate Osteochondral Mechanotransduction Pathways. 2014.
16. Linh NTB, Lee B-T. Electrospinning of polyvinyl alcohol/gelatin nanofiber composites and cross-linking for bone tissue engineering application. *Journal of biomaterials applications*. 2012;27(3): 255-66. [PubMed: 21680612]
17. Hoque ME, Nuge T, Yeow TK, Nordin N, Prasad R. Gelatin based scaffolds for tissue engineering- A review. *Polymers Research Journal*. 2015;9(1):15.
18. Liu D, Nikoo M, Boran G, Zhou P, Regenstein JM. Collagen and gelatin. *Annual review of food science and technology*. 2015;6:527-57.
19. ASTM. Standard Test Methods for Determination of Gel Content and Swell Ratio of Crosslinked Ethylene Plastics. West Conshohocken, PA: ASTM International; 2006.
20. Peppas NA, Wright SL. Solute Diffusion in Poly(vinyl alcohol)/Poly(acrylic acid) Interpenetrating Networks. *Macromolecules*. 1996;29(27):8798-804.
21. Mallapragada SK, Peppas NA. Dissolution mechanism of semicrystalline poly(vinyl alcohol) in water. *Journal of Polymer Science Part B: Polymer Physics*. 1996;34(7):1339-46.
22. Annabi N, Nichol JW, Zhong X, Ji C, Koshy S, Khademhosseini A, et al. Controlling the porosity and microarchitecture of hydrogels for tissue engineering. *Tissue Engineering Part B: Reviews*. 2010;16(4):371-83.
23. Pal K, Banthia AK, Majumdar DK. Preparation and characterization of polyvinyl alcohol-gelatin hydrogel membranes for biomedical applications. *Aaps Pharmscitech*. 2007;8(1):E142-E6.
24. Kozlov P, Burdygina G. The structure and properties of solid gelatin and the principles of their modification. *Polymer*. 1983;24(6):651-66.
25. Klouda L, Mikos AG. Thermoresponsive hydrogels in biomedical applications. *European Journal of Pharmaceutics and Biopharmaceutics*. 2008;68(1):34-45. [PubMed: 17881200]
26. Hassan CM, Peppas NA. Structure and morphology of freeze/thawed PVA hydrogels. *Macromolecules*. 2000;33(7):2472-9.
27. Zhang D, Duan J, Wang D, Ge S. Effect of preparation methods on mechanical properties of PVA/HA composite hydrogel. *Journal of Bionic Engineering*. 2010;7(3):235-43.
28. Anseth KS, Bowman CN, Brannon-Peppas L. Mechanical properties of hydrogels and their experimental determination. *Biomaterials*. 1996;17(17):1647-57. [PubMed: 8866026]
29. Zhang HJ, Xia HS, Zhao Y. Poly(vinyl alcohol) Hydrogel Can Autonomously Self-Heal. *ACS Macro Lett*. 2012;1(11):1233-6.

30. Sun TL, Kurokawa T, Kuroda S, Ihsan AB, Akasaki T, Sato K, et al. Physical hydrogels composed of polyampholytes demonstrate high toughness and viscoelasticity. *Nature materials*. 2013;12(10):932. [PubMed: 23892784]
31. Varshney L Role of natural polysaccharides in radiation formation of PVA–hydrogel wound dressing. *Nuclear Instruments and Methods in Physics Research Section B: Beam Interactions with Materials and Atoms*. 2007;255(2):343–9.
32. Aramwit P, Siritientong T, Kanokpanont S, Srichana T. Formulation and characterization of silk sericin–PVA scaffold crosslinked with genipin. *International journal of biological macromolecules*. 2010;47(5):668–75. [PubMed: 20804781]
33. Lim KS, Alves MH, Poole-Warren LA, Martens PJ. Covalent incorporation of non-chemically modified gelatin into degradable PVA-tyramine hydrogels. *Biomaterials*. 2013;34(29):7097–105. [PubMed: 23800741]

**Fig. 1.**

(A) SEM images of 15H-15-1 TC-gel surfaces after manufacturing compared to a cryo-fractured surface, showing the two distinct scales of porosity in the dehydrated hydrogel (x250 magnification, scale bar = 100  $\mu\text{m}$ ). (B) ATR-FTIR spectra of TC-gels and the respective controls. (C) Swell ratio and equilibrium water content calculated for TC-gels and the respective controls after 24 hours of hydration in DI water and subsequent lyophilization. Data are represented as mean  $\pm$  standard deviation;  $n = 5$ . (D) Images of Samples containing gelatin retained a pink hue, a signal that the Van Gieson's solution has bound to collagen, or in this case its gelatin derivative.

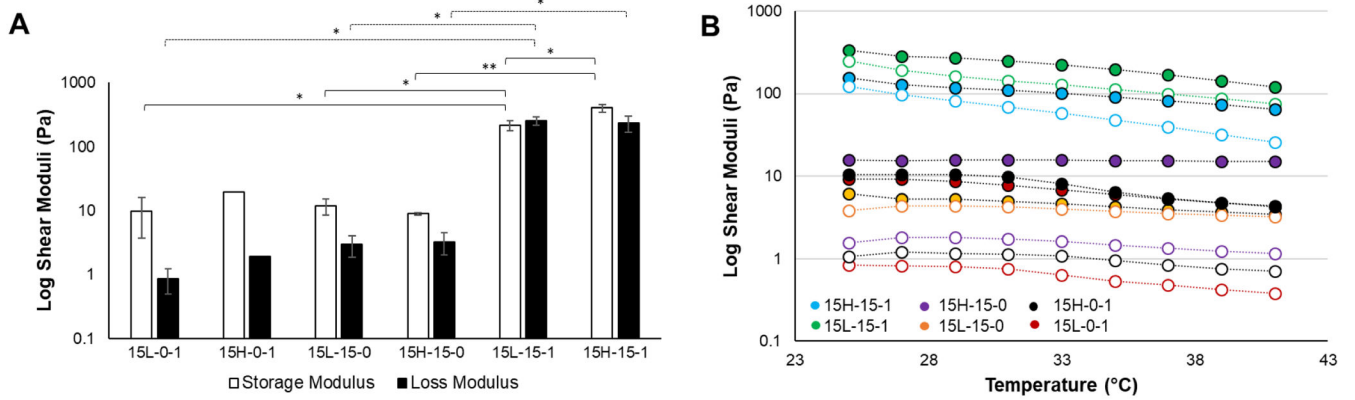


**Fig. 2.** (A) Bar graph depicting oscillatory shear moduli for the time sweep at room temperature (mean  $\pm$  standard deviation). Oscillatory time sweeps occurred at room temperature over a period of 3 minutes. There were no significant changes in the material with time; however, there were significant differences in  $G'$  and  $G''$  between groups (\*\*  $p < 0.01$ , \*  $p, 0.05$ ). (B) Oscillatory temperature sweeps from 25–41 °C. Samples containing gelatin showed a sharp decrease in modulus as temperature increased due to a conformational shift in the structure of gelatin, whereas those containing no gelatin saw no sharp change in modulus, (solid circles =  $G'$ , hollow circles =  $G''$ ).

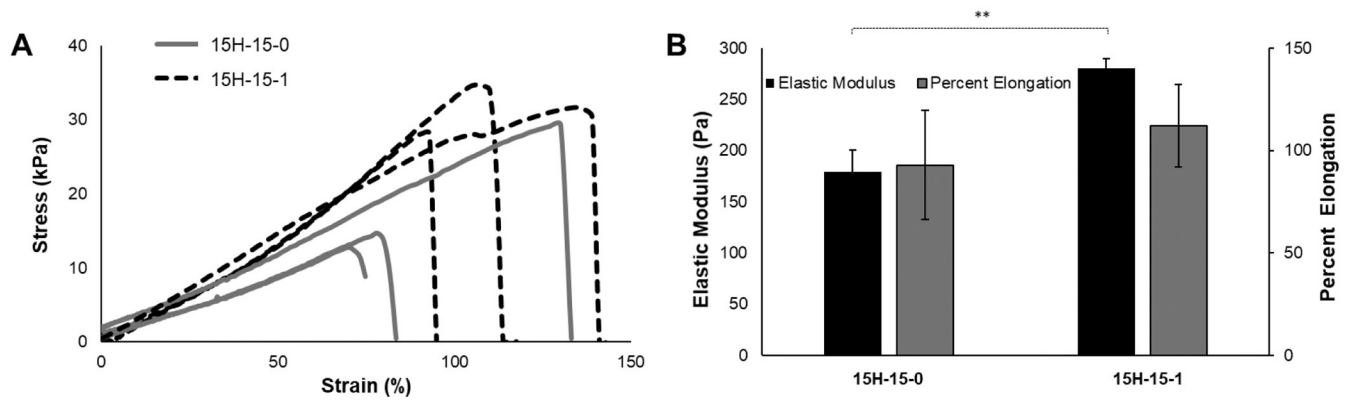


**Fig. 3.** (A) Stress versus percent elongation plots for the two tested material groups (\*\*  $p < 0.01$ ). (B) Average elastic modulus and percent elongation with standard deviation. There was no significant difference in percent elongation ( $p = 0.374$ ).

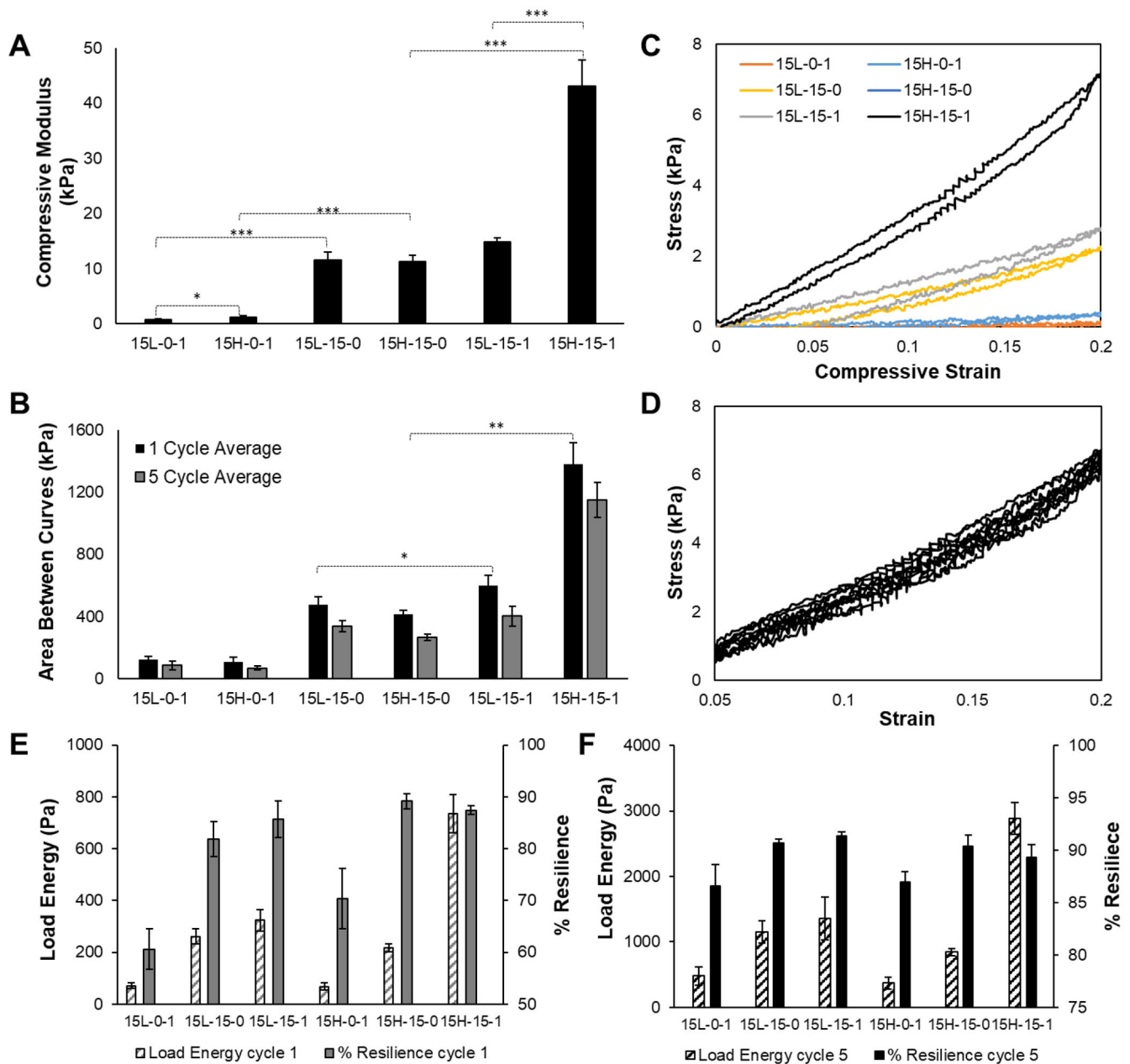


**Fig. 4.** (A) 0–20% uniaxial unconfined compression tests at 10  $\mu\text{m/s}$  (\*\*\*)  $p < 0.0001$ , \*  $p < 0.05$ ). (B) Average area between hysteresis curves with standard deviation. This area is indicative of energy loss between loading and unloading curves (\*\*  $p < 0.01$ , \*  $p < 0.05$ ). (C) 0–20% strain single cycle representative hysteresis curve for each material group. (D) 5–20% strain five cycle representative hysteresis curve for the 15H-15-1 material group. Dynamic data is also presented as (E) the total energy absorbed by the materials during loading and (F) the percent energy returned (i.e., % resilience) upon unloading.